A Mechanistic Study on the Catalytic, Asymmetric α-Bromination of Acid Chlorides

Cajetan Dogo-Isonagie,[a] Tefsit Bekele,[b] Stefan France,[c] Jamison Wolfer,[a] Anthony Weatherwax,[a] Andrew E. Taggi,[d] Daniel H. Paull,[a] Travis Dudding,[e] and Thomas Lectka*[a]

The mechanism of the catalytic, asymmetric α-bromination of acid chlorides is probed through a series of crossover experiments, ion-pairing tests, and kinetic resolution studies to shed light on the factors that contribute to, and limit the production of, optically-active α-bromo esters. In order to understand better the observed sense of induction, as well as the high degree of enantiomeric excess exhibited by these products, extensive molecular modeling is employed on the relevant transition states. Finally, the usefulness of the α-bromo ester products is demonstrated by their simple derivatization into chiral epoxides.

(© Wiley-VCH Verlag GmbH & Co. KGaA, 69451 Weinheim, Germany, 2007)

Introduction

We have previously documented a versatile catalytic, asymmetric process for the α-chlorination of acid halides employing cinchona alkaloid derivatives as catalysts in conjunction with various stoichiometric bases.[1] In the interest of fully understanding this methodology, we went on to conduct in-depth mechanistic studies and explore the utility of the products through substitution experiments.[2] We found that although the chiral α-chloro ester products were produced in high enantioselectivity and good chemical yields, their utility as synthetic intermediates was somewhat compromised by the fact that, at times, displacement of chlorine is difficult, resulting in sluggish reactivity and racemization. This led us to consider alkyl bromides, which are generally believed to be the most synthetically useful of the halides, and which often react through a pure S_N2 mechanism during nucleophilic displacements under mild conditions.[3] In addition, the brominated products themselves can be of interest, as with halomon (**1a**) and bromophycolide A (**1b**, Figure 1), two natural products displaying effectiveness against several human tumor cell lines.[4]
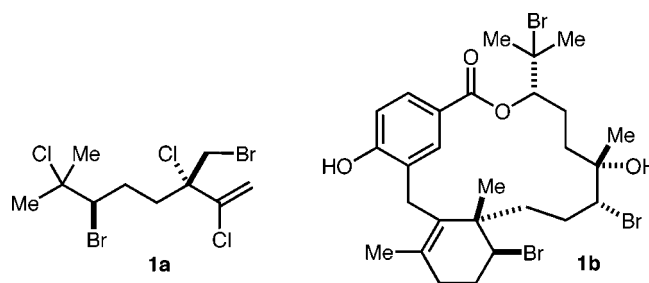

Figure 1. Examples of brominated natural products.

With a firm understanding of the chlorination mechanism in hand, we turned to the design of an analogous catalytic, asymmetric α-bromination of acid chlorides. As the research progressed, we realized that there were interesting mechanistic differences between the chlorination and bromination reactions. For example, our initial bromination conditions only worked well on a small scale.[5] Increasing the scale of the reaction, however, resulted in exponential loss of yield and enantioselectivity (*ee*). The chlorination reaction, on the other hand, displays no such erosion upon scale up. It became clear to us that in order to solve this scalability problem, we needed to understand in detail these mechanistic differences. This full account reports on the series of crossover experiments, ion-pairing tests, and kinetic resolution studies developed to explore, and provide insight into, the mechanism of our α-bromination reaction, and how it contrasts with our asymmetric α-chlorination.

Reaction Overview

We postulated that the general reaction sequence (Scheme 1) proceeds from the acid chloride starting mate-

[a] Department of Chemistry, New Chemistry Building, Johns Hopkins University,
3400 North Charles Street, Baltimore, MD 21218, USA
[b] Milliken & Co.,
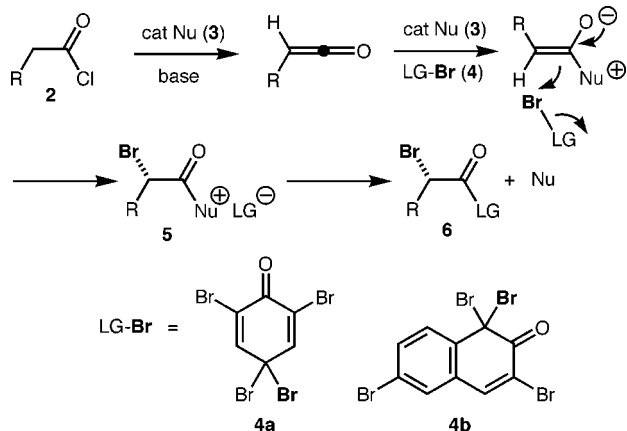1300 4th Avenue, LaGrange, GA 30240, USA
[c] Department of Chemistry, Emory University,
1515 Dickey Drive, Atlanta, GA 30322, USA
[d] DuPont Crop Protection, Stine-Haskell Research Center,
1090 Elkton Road, Newark, DE 19711, USA
[e] Department of Chemistry, Brock University,
500 Glenridge Avenue, St. Catharines, ON, Canada L2S 3A1, Canada
Supporting information for this article is available on the WWW under http://www.eurjoc.org or from the author.

rial **2**, to a zwitterionic enolate intermediate formed by the action of our catalyst **3** and a stoichiometric base. We believe that this transient, chiral nucleophile abstracts Br$^+$ from the brominating agent **4**, producing an ion-paired intermediate **5** that undergoes transacylation to produce the desired product **6** and regenerate the catalyst **3** for another cycle. The resulting optically enriched α-bromo esters are produced in high *ee* and moderate to good chemical yields.

line cinchona alkaloid conjugate, **3b**) to replace benzoyl quinine (BQ, **3a**, Figure 2); and (2) substituting *ortho*-brominating agent **4b** for *para*-brominating agent **4a** (Scheme 1),[6] in conjunction with changing the stoichiometric base from heterogeneous carbonates to homogeneous Hünig's base for aliphatic acid chlorides, or NaH solubilized by catalytic amounts of 15-crown-5 for arylacetyl chlorides.
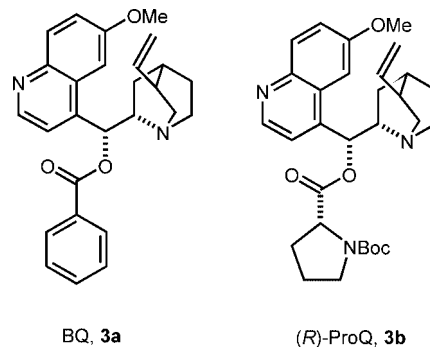

Scheme 1. Tandem catalytic, asymmetric bromination/esterification.

Figure 2. Catalysts tested.

1. Catalyst Optimization

As discussed previously, the initial bromination conditions had to be optimized to eliminate problems with loss of selectivity and yield upon scale up. These formerly reported optimization procedures involved: (1) development, through de novo design, of a more selective catalyst (a pro-

Although we had previously used BQ (**3a**) as a successful catalyst system,[7] it was evident to us that our catalyst was not sufficiently optimized for this application. We decided to turn to molecular mechanics (MM) to guide our substitution of the cinchona alkaloid core, a method that has served us well in the past.[8] Amino acids were a class of compounds we identified as possible modifiers for this de novo catalyst. Replacing the benzoyl group in BQ (**3a**), with
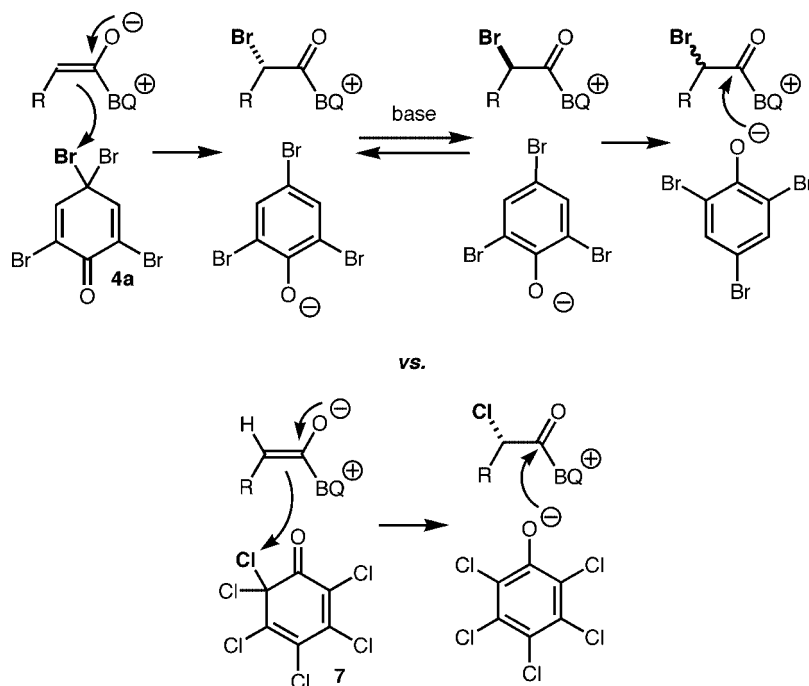
Scheme 2. Halogenating agent's effect on intermediate lifetime.

(*R*)-Boc-prolyl (**3b**) showed considerable promise in our MM study, revealing an increase in the gap between the low energy *re*- and *si*-face exposed confirmation relative to BQ, thus predicting improved selectivity.[6] This prediction was borne out experimentally (as **3b** gives an average of ten percent higher *ee* in our bromination reaction at increased scale).

2. Brominating Agent Development

Observations made during our early experiments led us to suspect that some racemization was occurring during the reaction process since stoichiometric bases such as NaH or K_2CO_3 were employed. If this were true, the species most susceptible to racemization would likely be the acyl ammonium intermediate (**5**, Scheme 1). Comparing our α-bromination reaction to its analogous α-chlorination led us to realize that **5** may be longer-lived in the α-bromination reaction as the phenolate counterion of the *para*-brominating agent **4a** must "wheel around" to capture the acyl ammonium salt. However, in the chlorination reaction, trapping would be more rapid because the phenolate oxygen is in the *ortho* position relative to the active site of the chlorinating agent, and thus perfectly positioned for transacylation. This longer-lived acyl ammonium intermediate in the α-bromination reaction would therefore be subject to racemization by adventitious bases (Scheme 2).

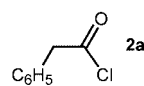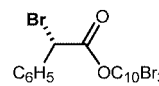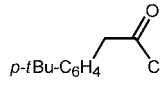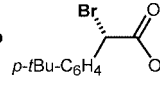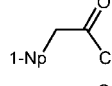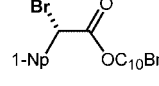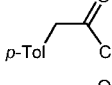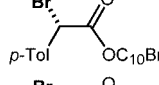As reported in our earlier publication,[6] this theory led us to synthesize brominating agent **4b** (Scheme 1), an *ortho*-polybromoquinone, in an effort to solve the racemization problem. Our initial hypothesis appears to be supported, by the fact that **4b** gave products with improved enantioselectivities upon testing.

Optimization Results

In a typical optimized procedure, phenylacetyl chloride (**2a**) was added to a stirred suspension of NaH and 10 mol-% each of 15-crown-5 and catalyst **3b** in THF at –78 °C. A THF solution of **4b** was then slowly added, and the reaction was stirred at –78 °C for 5 h before being quenched with methanolic HCl. Workup and column chromatography led to α-bromo ester **6a** in 55% yield and 99% *ee* (Table 1). A number of other arylacetyl chloride substrates were screened using the same procedure, and resulted in similar yields and good to excellent *ee* values (Table 1).
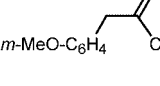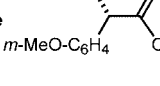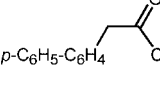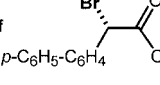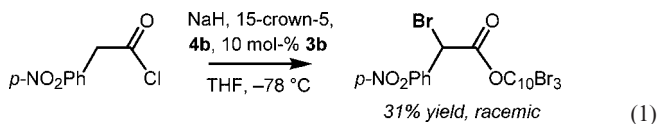
A limitation of the methodology, and also an interesting mechanistic clue, are seen when strong electron-withdrawing groups are present on the aromatic ring. For example, when *p*-nitrophenylacetyl chloride is subjected to the standard reaction conditions, substantial racemization is observed. The reaction proceeds in 31% yield with little or no selectivity [Equation (1)]. This loss of *ee* may be due to the increased acidity of the proton α to the carbonyl, and is also consistent with our mechanistic hypothesis.

Table 1. Catalytic, asymmetric α-bromination of arylacetyl chlorides.

Entry	Acid chloride	Product		% ee	% Yield[a]
1	C6H5, **2a**	C6H5, **Br**	(S)-**6a**	99	55
2	*p-t*Bu-C6H4, **2b**	*p-t*Bu-C6H4, **Br**	(S)-**6b**	92	54
3	1-Np, **2c**	1-Np, **Br**	(S)-**6c**	99	51
4	*p*-Tol, **2d**	*p*-Tol, **Br**	(S)-**6d**	96	46
5	*m*-MeO-C6H4, **2e**	*m*-MeO-C6H4, **Br**	(S)-**6e**	96	59
6	*p*-C6H5-C6H4, **2f**	*p*-C6H5-C6H4, **Br**	(S)-**6f**	83	44

[a] Reactions run with 10 mol-% catalyst **3b**, 0.609 mmol acid chloride, 0.522 mmol NaH, and 0.435 mmol **4b** at –78 °C for 5 h in THF; % yield based on brominating agent after chromatography.

$$p\text{-NO}_2\text{Ph} \quad \xrightarrow[\text{THF, –78 °C}]{\text{NaH, 15-crown-5,}\ \textbf{4b},\ 10\ \text{mol-\%}\ \textbf{3b}} \quad p\text{-NO}_2\text{Ph}\quad \text{OC}_{10}\text{Br}_3$$

31% yield, racemic   (1)

The reaction of aliphatic acid chlorides is similar to that of the arylacetyl chlorides. Addition of the acid chloride to a solution of one equiv. Hünig's base and 10 mol-% catalyst **3b** in THF at –78 °C was followed by the addition of a THF solution of brominating agent **4b**. The reaction was then stirred at –78 °C for 5 h before being quenched with methanolic HCl. Standard workup and column chromatography on Florisil® led to α-bromo esters in fair yield and good to excellent *ee*. For example, butyryl chloride (**2g**) was subjected to the above conditions to give **6g** in 44% yield and 99% *ee*. A number of other aliphatic substrates were also screened, as summarized in Table 2.

This optimized procedure has led to considerably improved scalability. While our original methodology produced good results on a small (≈ 25 mg) scale, enantioselectivities were seen to rapidly decay upon scale up.[5] Under our optimized conditions, we have conducted reactions on scales of up to 1 g without loss of selectivity or yield.[6]

Throughout the development of these optimized procedures, intriguing mechanistic questions continued to come to light, not the least of which is exactly why this reaction differs so significantly from the corresponding α-chlorination. The following sections outline our investigations into these questions.
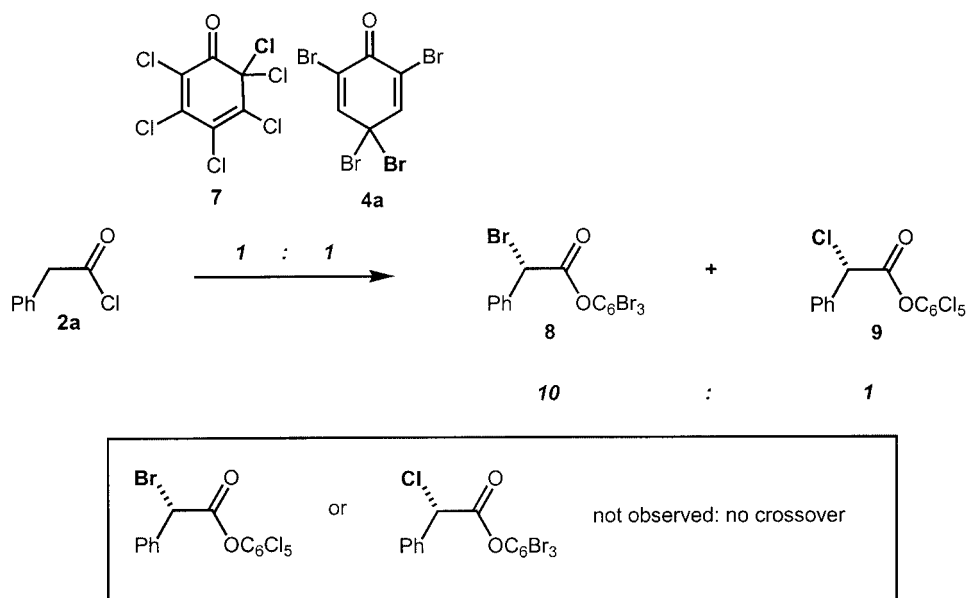
Table 2. Catalytic, asymmetric α-bromination of aliphatic acid chlorides.

Entry	Acid chloride	Product	% ee	% Yield[a]
1	2g	(S)-6g	99	44
2	2h	(S)-6h	99	41
3	2i	(S)-6i	92	41
4	2j	(S)-6j	6:1[b]	41
5	2k	(S)-6k	99	48
6	2l	(S)-6l	98	68

[a] Reactions run with 10 mol-% catalyst 3b, 0.522 mmol acid chloride, 0.435 mmol 4b, and 0.435 mmol Hünig's base at –78 °C for 5 h in THF. % Yield based on brominating agent after chromatography. [b] dr given in lieu of ee, β center not assigned.

Crossover Experiments

One issue that intrigued us concerns the extent to which free phenolate ions dissociate from the acyl ammonium salt after the halogen transfer step. For example, when we performed an asymmetric halogenation using 2a as substrate

and a 1:1 mixture of 4a and 7, we found only products 8 and 9 at all levels of conversion (Scheme 3). In general, the brominating agent 4a is about 10 times as reactive as the chlorinating agent 7 in THF solvent at –78 °C. No crossover products, which would arise from phenolate/acyl ammonium salt dissociation, were observed in the experiment, as determined by a fairly sensitive mass spectrometry assay and NMR spectroscopy.[9]

Ion Pairing and Dissociation

How may we address experimentally the role that ion pairing and/or dissociation plays in racemization? Because we postulate that long-lived ion-paired (or dissociated ion)
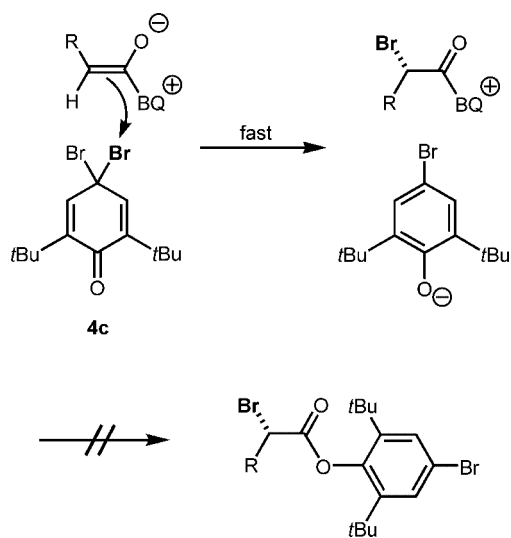
Scheme 4. The effect of a hindered brominating reagent.

Scheme 3. Crossover experiments.

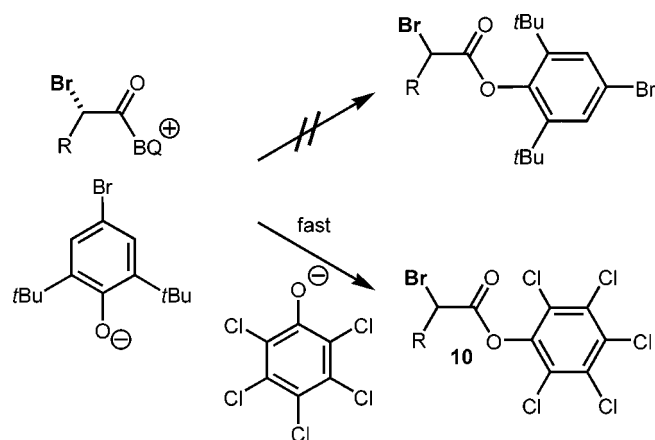intermediates may lead to racemization, a bulky brominating agent (especially one that can transfer bromine fast but transacylate slowly) should therefore lead to lower selectivities. For example, the reagent **4c**, derived from 2,6-di-*tert*-butylphenol,[10] would lead to the ion-pair intermediate shown in Scheme 4. The steric hindrance of the two *ortho* *tert*-butyl groups should slow down the rate of transacylation considerably, allowing the acyl ammonium salt to accumulate in solution and therefore racemize.

Upon conducting the experiment, we found that brominating agent **4c** provided little or no desired product in a standard reaction employing NaH as the stoichiometric base. Presumably, whereas bromination from the unhindered para position may occur readily, transacylation is prevented, precluding product formation and catalyst turnover.

What then about the possibility of an added "co-nucleophile" that can take the place of the 2,6-di-*tert*-butylphenolate as a transacylating agent? In fact, to our surprise, running the standard reaction in the presence of 1 equiv. of sodium pentachlorophenolate does indeed produce a satisfactory yield of product **10** by promoting transacylation and catalyst turnover (Scheme 5). However, if our hypothesis about ion pair lifetimes is correct, the enantioselectivity of the product should be diminished, as a new ion pairing between the ammonium salt and pentachlorophenolate must presumably be established before product formation can take place (Scheme 6). The intervening time may be

thus long enough for racemization to take place. In fact, our hypothesis is confirmed by experiment, as the resulting product is *virtually racemic*.
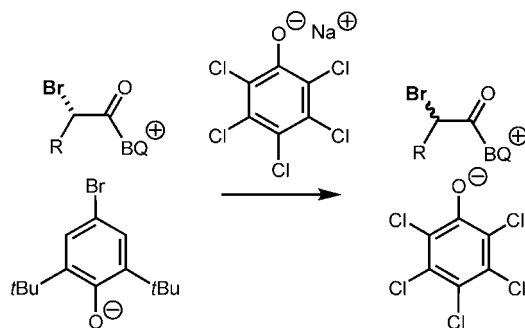
Scheme 6. Ion-pair swapping.

To ensure that this reaction (Scheme 5) is not occurring via an alternate mechanism where pentachlorophenolate would catalyze the formation of crossover product **10** by forming a pentachlorophenol enolate, a simple control was set up without the chiral catalyst BQ (**3a**). No crossover product **10** was observed [Equation (2)].

(2)
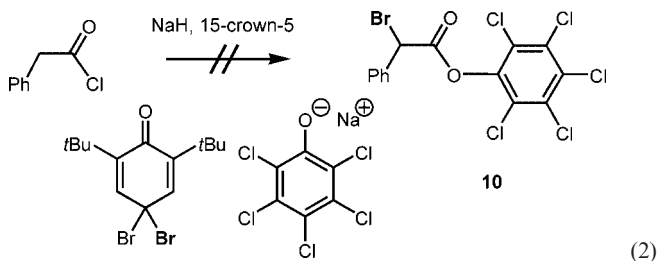
The question of why this racemization occurs so readily can be addressed by further experimentation. Racemic α-bromophenylacetyl chloride was treated with tribromophenol in the presence of BQ and Hünig's base. The product **8** was recovered in a racemic form in all tests. The lack of any kinetic resolution effect in this reaction suggests that only a small difference in energy exists between the diastereomeric acylammonium intermediates (Scheme 7).[11]

Scheme 5. Nucleophilic capture of a reactive intermediate.
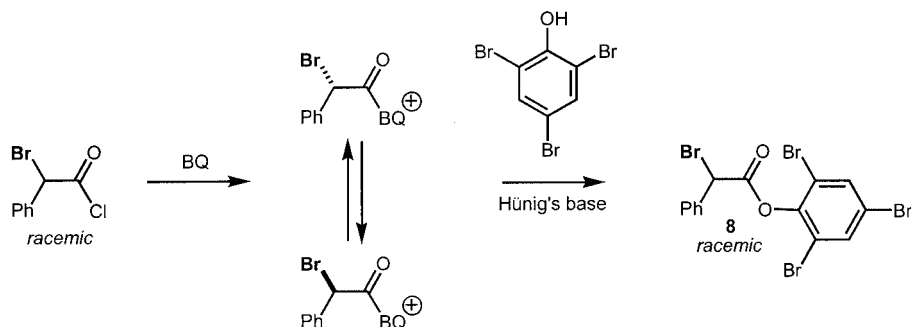
Scheme 7. Kinetic resolution study.

no detected product

trace product
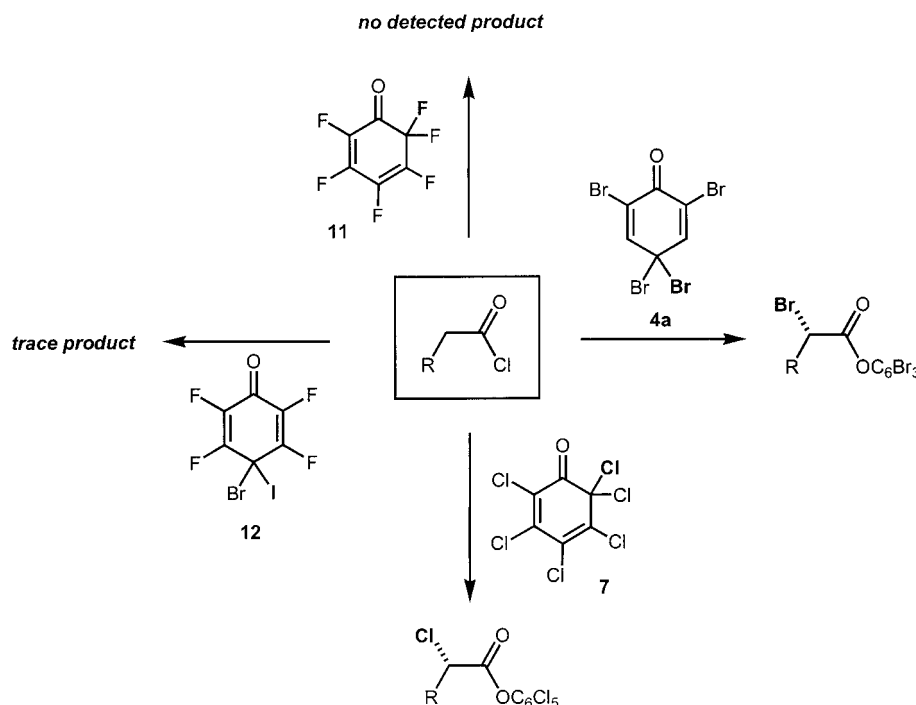
Scheme 8. Reactivities of halogenating agents.

Window of Reactivity

The issues of ion-pair swapping and transacylation discussed above demonstrate that it can be illustrative to compare the reactivity of our various quinone-based halogenating agents. The effects of differing carbon–halogen bond strengths, coupled with quinone ring substituents and geometry combine to produce a spectrum of reactivity. Under no circumstances is fluorine transfer observed when quinone (11) is employed,[12] while chlorine transfer is well established, and bromine transfer is even faster. Iodine transfer, however, occurs only with very low efficiency;[13] a fact that results from the extreme reactivity (and poor selectivity) of the iodinating agent 12 that readily transfers iodine to the solvent medium (Scheme 8).

Computational Studies

In order to gain further insight into the factors contributing to our observed sense of induction and degree of enantiomeric excess, we turned to molecular modeling. In our previous work on catalytic, enantioselective β-lactam formation we had employed such studies with great success, obtaining results that were in good agreement with experimental results, and which shed additional light on the reaction mechanisms involved.[14] Particularly, we felt that the application of modeling here might help explain the decrease in enantioselectivity observed when a employing para-brominating agent.

To investigate how catalyst 3a may be inducing selectivity in its reaction with phenylketene and brominating agent 4b, the low energy si- and re-transition states, TS1 and TS2,

were computed (Figure 3).[15] All calculations were carried out using the Gaussian 03 program[16] and MCMM searches were performed with Macromodel 7.1.[17] The short carbon–bromine bonds of the enolate, and the correspondingly longer carbon–bromine bonds of the quinone, are consistent with halogen transfer occurring late on the reaction coordinate, which is in turn consistent with a highly enantioselective reaction.[18] The most striking feature of the late transition states TS1 and TS2 is stabilization of the developing phenolate through polarized $O\delta^-\cdots H\delta^+ - C\delta^-$ hydrogen bonding. Of specific interest in this regard are the bridging contacts between the phenolate oxygen and quinuclidine nucleus (printed in blue).[19] Based on calculated Mulliken charges,[20] the quinuclidine hydrogens involved in this interaction hold the highest Lewis acidity. In a similar fashion, the ketene enolate appears to be stabilized by favorable contacts with the proximal hydrogen atoms of the catalyst's quinuclidine ring, as judged from the relatively short O⁻···H contact distances[21] (printed in red).

A closer look at TS2 reveals a second factor leading to the 1.6 kcal/mol energetic preference for si-addition. A repulsive van der Waals contact between the enolate α-hydrogen and the C–H hydrogen α to the benzoyl group of the catalyst (printed in purple) destabilizes TS2. The measured length of this unfavorable contact is 2.0 Å, which lies well within the sum of the independent hydrogen radii (2.2 Å). These unfavorable steric interactions are lessened in TS1, suggesting a lower energy barrier for si-addition. In fact, the calculated enantioselectivity of 87% ee, derived from the computed IMOMO energies, is in close agreement with the experimental value of 88% ee for BQ-catalyzed bromination of phenyl ketene with brominating agent 4b.
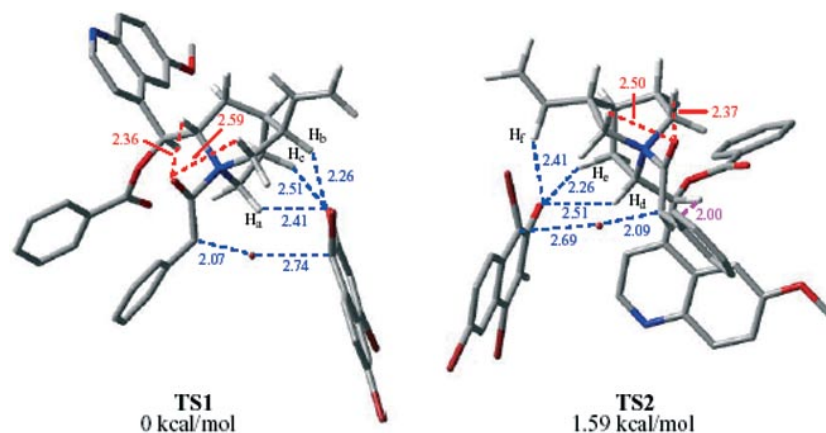
Figure 3. Low energy enantioselective *si*- and *re*-transition states TS1 and TS2 for the benzoylquinine **3a** catalyzed bromination of phenylketene by halogenating reagent **4b**.[22]
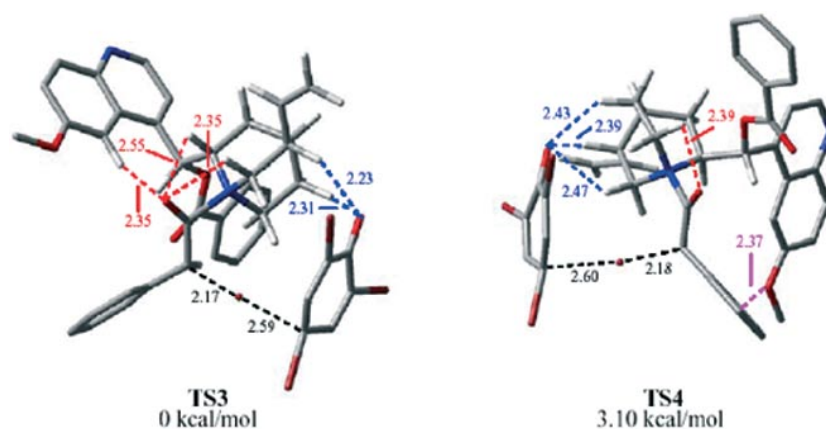

Figure 4. Low energy enantioselective *si*- and *re*-transition states TS3 and TS4 for benzoylquinine **3a** catalyzed bromination of phenyl ketene by halogenating reagent **4a**.[28]

In light of the above result, a similar study was performed for *para*-dibromo-substituted **4a** in its reaction with catalyst **3a** and phenyl ketene (Figure 4). Transition states **TS3** and **TS4** can be seen to share similar geometries to those found in **TS1** and **TS2**.[23] The preference for **TS3** can be explained by two distinct interactions. **TS3** benefits from a 3-point hydrogen-bond network between the proximal quinuclidine ring hydrogen atoms of the catalyst and the enolate oxygen (*printed in red*).[24] In contrast, **TS4** possesses only one such favorable hydrogen-bond contact (*printed in red*). Also, like **TS2**, **TS4** suffers from a destabilizing van der Waals contact (2.37 Å) between the ketene enolate phenyl ring and the methoxy ether oxygen of the catalyst′s quinoline ring (*printed in purple*). With the above in mind, and further application of computed IMOMO energies, the model predicts a product with (*S*)-stereochemistry and 98.9% *ee*. While the sense of induction predicted is correct, the experimentally observed enantiomeric excess (78%) is significantly lower than that obtained via computation.

Molecular Dynamics Study

The aforementioned discrepancy between predicted and observed selectivities, and the overall lower enantioselectivity obtained with brominating reagent **4a** (as opposed to that obtained with **4b**) can be explained by the competition between epimerization of the acyl ammonium intermediate and phenolate transacylation. Following this rationale, and taking into account the respective transition state geometries, we anticipated that the time required for transacylation should be greater for a phenolate generated from **4a** than one generated from **4b**. To explore this possibility, a series of stochastic dynamics simulations were performed using preferred transition states **TS1** and **TS3** as starting geometries (Figure 5 and Figure 6, respectively).[25]

We monitored trajectories for the reactions of **4a** and **4b** with a prototype ketene enolate. In particular, the phenolate anion of **4a** was found to require more than twice as much time (8.5 ps vs. 3.6 ps for **4b**) to obtain a ground-state geom-
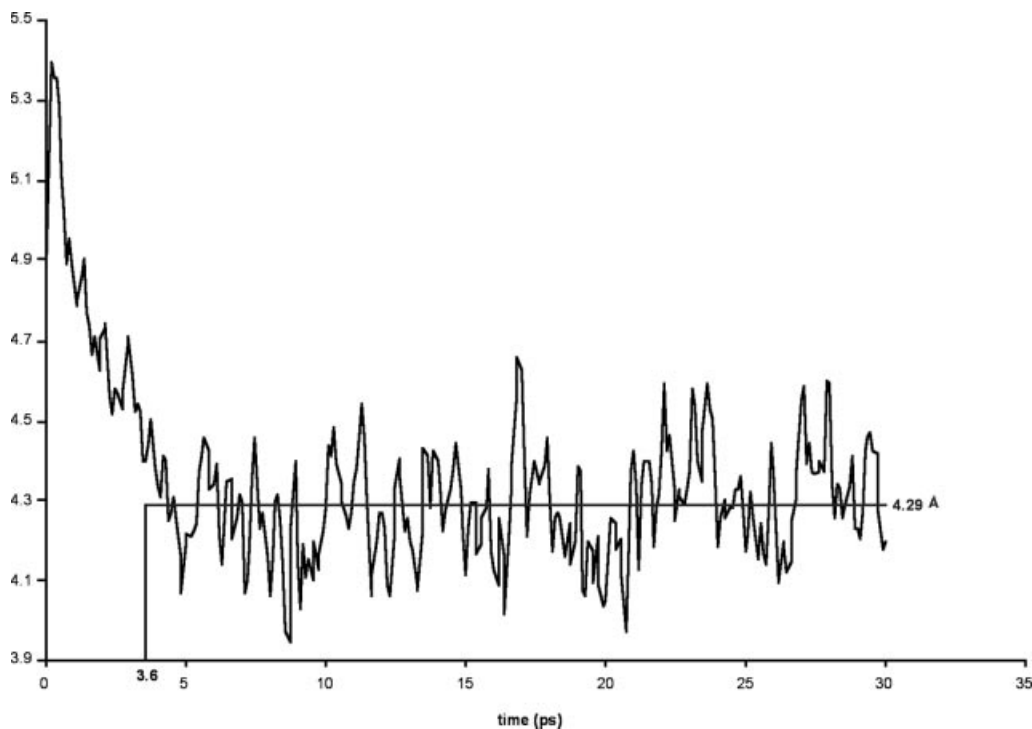
Figure 5. Trajectory plot of the time required for the phenolate anion of **4b** to obtain an O···C=O distance suitable for transacylation. The horizontal line overlaid on the plot represents the average distance of the phenolate oxygen from the acylammonium carbonyl carbon. The first data point at which the average distance for transacylation is obtained during the 30 ps simulation is marked by a vertical line.

Figure 6. Trajectory plot of the time required for the phenolate anion of **4a** to obtain an O⁻···C=O distance suitable for transacylation. The horizontal line overlaid on the plot represents the average distance of the phenolate oxygen from the acylammonium carbonyl carbon. The first data point at which the average distance for transacylation is obtained during the 30 ps simulation is marked by a vertical line.
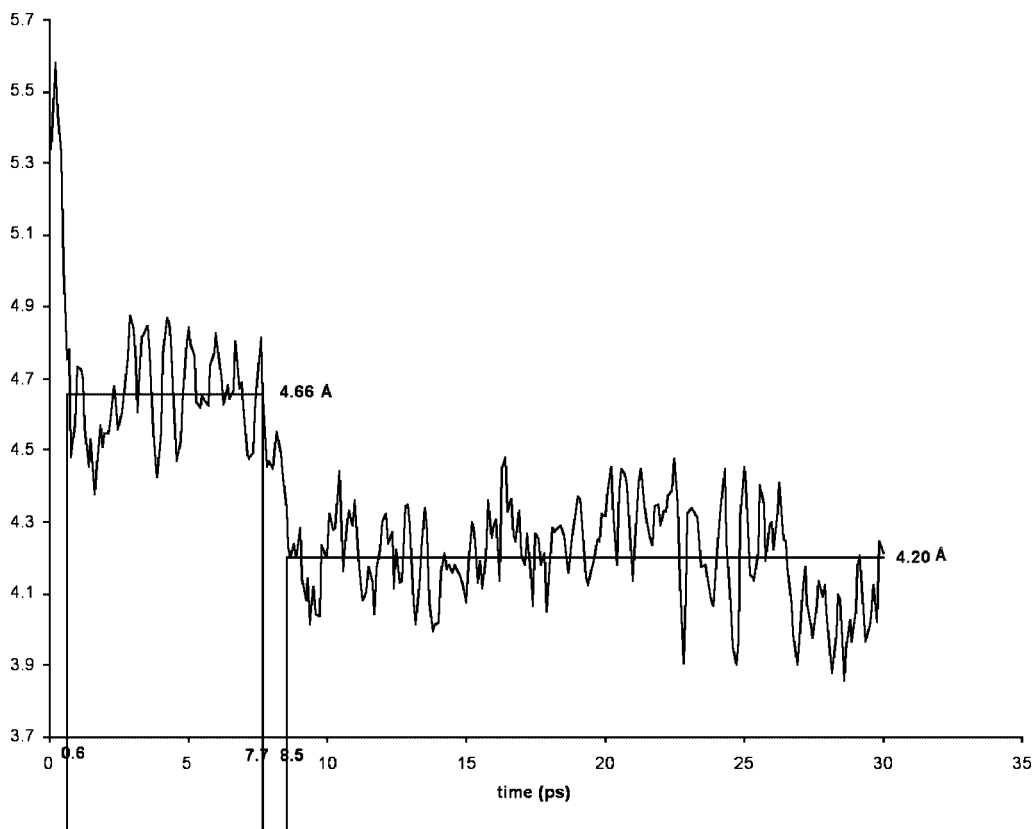
etry [one having O⁻···C=O distances suitable for transacylation (4.20 Å and 4.29 Å, respectively)], than the phenolate derived from **4b**.[26] One contributing factor to this rate disparity is the positioning of the phenolic oxygen, *ortho* in **4b** and *para* in **4a**. Another, less obvious, strike against **4a** is that transacylation by its phenolate appears to be further slowed as a result of F-strain generated by the bromine atoms *ortho* to the oxygen.[27]

When these computational studies and molecular dynamics calculations are taken together, a complex picture of the halogenation reaction emerges, one supported by our experimental findings. While the enantioselectivity of a given product is determined initially by interaction with the catalyst, the final enantiomeric excess is strongly influenced by the interplay of a dynamic process, one balancing epimerization (leading to product racemization) against transacylation.

Terminal Epoxide Formation by Bromine Displacement

As mentioned previously, the displacement of bromine by a variety of nucleophiles is readily accomplished as the reaction proceeds through a pure S_N2 mechanism under mild conditions. A practical use for our α-bromo ester products is the facile synthesis of optically active, terminal epoxides. Chiral epoxide chemistry has been a topic of intense interest for a generation, and some of the most notable advances in asymmetric catalysis have been made in this area.[28] That being said, several challenges remain. Among the most notable is the catalytic, asymmetric synthesis of terminal epoxides. Jacobsen has addressed the problem from one angle by a catalytic, asymmetric hydrolytic resolution of chiral epoxides.[29] Our strategy is simple – a reduction of the optically enriched α-bromo ester is followed by simple, base-promoted cyclization to the epoxide.[30]

As a proof of principle, we performed this reaction sequence on the α-bromo ester **13**. After conversion to the corresponding alcohol **14** by NaBH₄, displacement of bromine, by an intramolecular cyclization to form the chiral epoxide **15** was accomplished by treatment of the alcohol with KOH under ambient conditions.[31] The reaction proceeded in approximately 80% yield and with full retention of enantioselectivity [Equation (3)].[32]

(3)
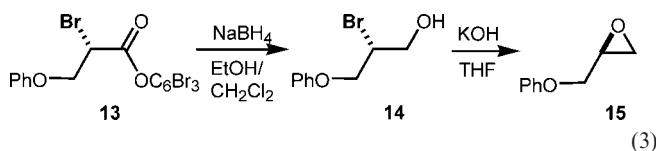
Conclusions

We have reported numerous reactivity, crossover, and ion-pairing experiments, supported by relevant computa-

tional and molecular mechanics studies that were employed to shed light on the mechanism of our α-bromination reaction. The utility of the corresponding α-bromo ester products as synthetic intermediates was demonstrated by the synthesis of a terminal chiral epoxide with no loss in enantioselectivity.

Experimental Section

Representative Bromination Procedure for Arylacetyl Substrates

1,3,6-Tribromo-2-naphthyl (S)-2-Bromo-2-phenylacetate (6a): A solution of phenylacetyl chloride (**2a**) (0.609 mmol) in 1 mL THF was added dropwise to a stirred suspension of catalyst **3b** (0.044 mmol), 15-crown-5 (0.044 mmol), and sodium hydride (0.522 mmol) in 3 mL THF at –78 °C. Next, a solution of **4b** (0.435 mmol) in 3 mL THF was added dropwise over 5 min. The resulting solution was stirred for 5 h at –78 °C. The reaction mixture was then quenched with methanolic HCl (4 drops of HCl in 3 mL methanol) and extracted three times with Et₂O. The organic layers were combined, dried with MgSO₄, and purified by column chromatography (100% hexanes) to yield **6a** in 55% yield. White crystalline solid (analytical sample was recrystallized from hexanes): m.p. 114 °C. $[a]_{25}$ = +45 (c = 0.01, CHCl₃). ¹H NMR (CDCl₃): δ = 8.0–7.9 (m, 3 H), 7.7–7.6 (m, 3 H), 7.4 (m, 3 H), 5.7 (s, 1 H) ppm. ¹³C NMR (CDCl₃): δ = 164.78, 143.52, 134.63, 133.64, 133.64, 131.61, 130.77, 130.26, 129.82, 129.71, 129.21, 129.16, 129.01, 128.93, 122.03, 116.15, 45.77 ppm. IR (CH₂Cl₂): ṽ = 1775 cm⁻¹. C₁₈H₁₀Br₄O₂ (577.86): calcd. C 37.41, H 1.74, Br 55.31, O 5.54; found C 37.38, H 1.79, Br 55.28, O 5.55.

Representative Bromination Procedure for Aliphatic Substrates

1,3,6-Tribromo-2-napthyl (S)-2-Bromo-3-phenylpropanoate (6k): A solution of dihydrocinnamoyl chloride (**2k**) (0.522 mmol) in 1 mL THF was added dropwise to a stirred solution of catalyst **3b** (0.044 mmol) and Hünig's base (0.435 mmol) in 3 mL THF at –78 °C. Next, a solution of **4b** (0.435 mmol) in 3 mL THF was added dropwise over 5 min. The resulting solution was stirred for 5 h at –78 °C. The reaction mixture was then quenched with methanolic HCl (4 drops of HCl in 3 mL methanol) and extracted three times with Et₂O. The organic layers were combined, dried with MgSO₄, and purified by column chromatography (100% hexanes) to yield **6k** in 48% yield. White crystalline solid (analytical sample was recrystallized from hexanes): m.p. 130 °C. $[a]_{25}$ = –0.56 (c = 0.01, CHCl₃). ¹H NMR (CDCl₃): δ = 8.0 (m, 2 H), 7.9 (m, 1 H), 7.6 (d, 1 H), 7.3 (m, 5 H), 4.8 (dd, 1 H), 3.7 (dd, 1 H), 3.4 (dd, 1 H) ppm. ¹³C NMR (CDCl₃): δ = 166.00, 143.54, 136.32, 133.771, 132.01, 131.60, 130.74, 130.34, 129.73, 129.13, 128.80, 127.53, 122.01, 117.16, 116.21, 43.68, 41.06 ppm. IR (CH₂Cl₂): ṽ = 1776 cm⁻¹. Anal Calcd for C₁₉H₁₂Br₄O₂ (591.91): calcd. C 38.55, H 2.04, Br 54.00, O 5.41; found C 38.51, H 2.09, Br 54.02, O 5.38.

Supporting Information (see also the footnote on the first page of this article): Contains general procedures for the synthesis of α-halo esters, brominating agents, and catalysts; compound characterization data; and reaction conditions for all crossover experiments and mechanistic studies.

Acknowledgments

[1] a) H. Wack, A. E. Taggi, A. M. Hafez, W. J. Drury, T. Lectka, *J. Am. Chem. Soc.* **2001**, *123*, 1531–1532; b) S. France, A. Weatherwax, T. Lectka, *Eur. J. Org. Chem.* **2005**, *3*, 475–479. For other examples of α-chlorination reactions see: c) D. A. Evans, J. A. Ellman, R. L. Dorrow, *Tetrahedron Lett.* **1987**, *28*, 1123–1126; d) M. P. Brochu, S. P. Brown, D. W. C. MacMillan, *J. Am. Chem. Soc.* **2004**, *126*, 4108–4109; e) S. Bertelsen, N. Halland, S. Bachmann, M. Marigo, A. Braunton, K. A. Jørgensen, *Chem. Commun.* **2005**, *126*, 4821–4823; f) N. Shibata, J. Kohno, K. Takai, T. Ishimaru, S. Nakamura, T. Toru, S. Kanemasa, *Angew. Chem. Int. Ed.* **2005**, *44*, 4204–4207; g) L. Hintermann, A. Togni, *Helv. Chim. Acta* **2000**, *83*, 2425–2435. For a recent review see; h) M. Oestreich, *Angew. Chem.; Int. Ed.* **2005**, *44*, 2324–2327.

[2] S. France, H. Wack, A. E. Taggi, A. M. Hafez, T. R. Wagerle, M. H. Shah, C. L. Dusich, T. Lectka, *J. Am. Chem. Soc.* **2004**, *126*, 4245–4255.

[3] a) F. D'Angeli, P. Marchetti, V. Bertolasi, *J. Org. Chem.* **1995**, *60*, 4013–4016; b) M. Seki, T. Yamanaka, K. Kondo, *J. Org. Chem.* **2000**, *65*, 517–522.

[4] Halomon: a) R. W. Fuller, J. H. Cardellina II, J. Jurek, P. J. Scheuer, B. Alvarado-Lindner, M. McGuire, G. N. Gray, J. R. Steiner, J. Clardy, E. Menez, R. H. Shoemaker, D. J. Newman, K. M. Snader, M. R. Boyd, *J. Med Chem.* **1994**, *37*, 4407–4411. Bromophycolide A: b) J. Kubanek, A. C. Prusak, T. W. Snell, R. A. Giese, K. I. Hardcastle, C. R. Fairchild, W. Aalbersberg, C. Raventos-Suarez, M. E. Hay, *Org. Lett.* **2005**, *7*, 5261–5264.

[5] A. M. Hafez, A. E. Taggi, H. Wack, J. Esterbrook, T. Lectka, *Org. Lett.* **2001**, *3*, 2049–2051.

[6] C. Dogo-Isonagie, T. Bekele, S. France, J. Wolfer, A. Weatherwax, A. E. Taggi, T. Lectka, *J. Org. Chem.* in press.

[7] A. E. Taggi, A. M. Hafez, H. Wack, B. Young, D. Ferraris, T. Lectka, *J. Am. Chem. Soc.* **2002**, *124*, 6626–6636.

[8] A. E. Taggi, A. M. Hafez, T. Dudding, T. Lectka, *Tetrahedron* **2002**, *58*, 8351–8356.

[9] See Supporting Information for details.

[10] L. A. Paquette, G. J. Hefferon, R. Samodral, Y. Hanzawa, *J. Org. Chem.* **1983**, *48*, 1262–1266.

[11] Molecular mechanics calculations confirm that there is a less than 0.5 kcal/mol difference between the diastereomeric acyl-ammonium intermediates.

[12] R. R. Soelch, G. W. Mauer, D. M. Lemal, *J. Org. Chem.* **1985**, *50*, 5845–5852.

[13] L. Denivelle, H. A. Hoa, *Bull. Soc. Chim. Fr.* **1974**, 2171–2174.

[14] A. E. Taggi, A. M. Hafez, T. Dudding, T. Lectka, *Tetrahedron* **2002**, *58*, 8351–8356.

[15] A combination of IMOMO (integrated molecular orbital + MO method) variation of ONIOM (n-layered integrated molecular orbital method) at the HF3-21G(d)//AM1 level, coupled with constrained Monte-Carlo conformational searches (MCMM) to generate initial IMOMO geometries.

[16] M. J. Frisch, G. W. Trucks, H. B. Schlegel, G. E. Scuseria, M. A. Robb, J. R. Cheeseman, J. A. Montgomery, Jr., T. Vreven, K. N. Kudin, J. C. Burant, J. M. Millam, S. S. Iyengar, J. Tomasi, V. Barone, B. Mennucci, M. Cossi, G. Scalmani, N. Rega, G. A. Petersson, H. Nakatsuji, M. Hada, M. Ehara, K. Toyota, R. Fukuda, J. Hasegawa, M. Ishida, T. Nakajima, Y. Honda, O. Kitao, H. Nakai, M. Klene, X. Li, J. E. Knox, H. P. Hratchian, J. B. Cross, C. Adamo, J. Jaramillo, R. Gomperts, R. E. Stratmann, O. Yazyev, A. J. Austin, R. Cammi, C. Pomelli, J. W. Ochterski, P. Y. Ayala, K. Morokuma, G. A. Voth, P. Salvador, J. J. Dannenberg, V. G. Zakrzewski, S. Dapprich, A. D. Daniels, M. C. Strain, O. Farkas, D. K. Malick, A. D. Rabuck, K. Raghavachari, J. B. Foresman, J. V. Ortiz, Q. Cui, A. G. Baboul, S. Clifford, J. Cioslowski, B. B. Stefanov, G. Liu, A. Liashenko, P. Piskorz, I. Komaromi, R. L. Martin, D. J. Fox, T. Keith, M. A. Al-Laham, C. Y. Peng, A. Nanayakkara, M. Challacombe, P. M. W. Gill, B. Johnson, W. Chen, M. W. Wong, C. Gonzalez, J. A. Pople, *Gaussian 03*, revision B. 04, Gaussian, Inc., Pittsburgh, PA, **2003**.

[17] Macromodel V. 8.6 copyright© **2004**, Schrödinger, LLC.

[18] The enolate carbon–bromine distances are 2.07 Å in **TS1** and 2.09 Å in **TS2**. The quinone carbon–bromine distances are 2.69 Å in **TS1** and 2.74 Å in **TS2**.

[19] These bonds have measured distances of 2.26 Å, 2.41 Å, and 2.51 Å in **TS1**; and 2.28 Å, 2.29 Å, and 2.51 Å in **TS2**.

[20] The calculated Mulliken charges are: H_a = +0.25, H_b = +0.23, and H_c = +0.21 in **TS1**; and H_d = +0.24, H_e = +0.22, and H_f = +0.21 in **TS2**.

[21] The ketene enolate oxygen–quinuclidine hydrogen distances are 2.37 Å and 2.51 Å in **TS1** and, 2.36 Å and 2.51 Å in **TS2**.

[22] Final energies represent ΔE values computed using the IMOMO method at the HF3-21G(d)//AM1 level. Reported Mulliken charges were determined at the B3LYP/6-31(d) level of theory through single-point calculations using optimized IMOMO geometries. Select hydrogens have been removed for simplicity.

[23] Among these are elongated quinone⋯Br bond lengths of 2.59 Å and 2.60 Å, and short enolate⋯Br distances of 2.17 Å and 2.18 Å, which are consistent with halogen transfer occurring late on the reaction coordinate.

[24] These hydrogen bonds have measured distances of 2.34 Å, 2.35 Å and 2.55 Å. For a related discussion regarding the strength of R_3N^+–C–H⋯O=C hydrogen bond interactions, see: C. E. Cannizzaro, K. N. Houk, *J. Am. Chem. Soc.* **2002**, *124*, 7163–7169.

[25] Stochastic molecular dynamics simulations performed using the MMFFs force field as implemented in Macromodel 7.1. The plotted trajectories represent the average values obtained from 5 independent simulations conducted at 195.15 K and 1 atm in vacuo. Initial equilibration and minimizations were not performed due to the instability associated with transition state geometries being potential energy maxima on the reaction surface.

[26] For a discussion on reaction trajectories for addition to carbonyls, see: H. B. Buergi, J. D. Dunitz, *Acc. Chem. Res.* **1983**, *16*, 153–161.

[27] a) H. C. Brown, M. D. Taylor, M. Gerstein, H. Bartholomay, *J. Am. Chem. Soc.* **1944**, *66*, 431–435; b) H. C. Brown, *Science* **1946**, *103*, 385; c) H. C. Brown, M. D. Talyor, *J. Am. Chem. Soc.* **1947**, *69*, 1332–1336.

[28] Recent reviews of asymmetric epoxidation: a) C. L. Winn, V. K. Aggarwal, *Acc. Chem. Res.* **2004**, *37*, 611–620; b) C. L. Winn, V. K. Aggarwal, *Acc. Chem. Res.* **2004**, *37*, 497–505; c) K. B. Sharpless, *Angew. Chem. Int. Ed.* **2002**, *41*, 2024–2032.

[29] L. P. C. Nielsen, C. P. Stevenson, D. G. Blackmond, E. N. Jacobsen, *J. Am. Chem. Soc.* **2004**, *126*, 1360–1362.

[30] MacMillan has reported the conversion of α-chloroaldehydes to optically enriched epoxides. Our approach is complementary; if you start with an aldehyde, use the MacMillan approach; if you start with a carboxylic acid, ester, or acid halide, our way may be chosen, as inexpensive commercial sources of all of these classes of compounds abound. See ref.[1e].

[31] S. Takano, T. Sugihara, T. Kamikubo, K. Ogasawara, *Heterocycles* **1991**, *32*, 1587–1591.

[32] Epoxide *ee* based on optical rotation. E. W. Collington, H. Finch, J. G. Montana, R. J. K. Taylor, *J. Chem. Soc., Perkin Trans. 1* **1990**, *7*, 1839–1843.